

# Prevention of Transthyretin Amyloid Disease by Changing Protein Misfolding Energetics

Per Hammarström,\* R. Luke Wiseman,\* Evan T. Powers, Jeffery W. Kelly†

Genetic evidence suggests that inhibition of amyloid fibril formation by small molecules should be effective against amyloid diseases. Known amyloid inhibitors appear to function by shifting the aggregation equilibrium away from the amyloid state. Here, we describe a series of transthyretin amyloidosis inhibitors that functioned by increasing the kinetic barrier associated with misfolding, preventing amyloidogenesis by stabilizing the native state. The trans-suppressor mutation, threonine 119 → methionine 119, which is known to ameliorate familial amyloid disease, also functioned through kinetic stabilization, implying that this small-molecule strategy should be effective in treating amyloid diseases.

Hundreds of human diseases, including the amyloidoses, are associated with protein misfolding (1–5). The 80 familial mutations that exacerbate [for example, Val<sup>30</sup> → Met<sup>30</sup> (V30M) and Leu<sup>55</sup> → Pro<sup>55</sup> (L55P) (6)] or ameliorate [Thr<sup>119</sup> → Met<sup>119</sup> (T119M) (7–9)] transthyretin (TTR) amyloid pathology (10) provide valuable mechanistic insights (11–13). All disease-associated mutations characterized thus far destabilize the TTR tetramer, and many influence the velocity of rate-limiting tetramer dissociation, with rapid

rates accelerating and slow rates retarding amyloidosis (11). We took advantage of the mechanism by which T119M prevents disease in V30M compound heterozygotes to develop small-molecule TTR amyloid inhibitors that dramatically slowed the initial misfolding event (tetramer dissociation) required for partial monomer denaturation, enabling misassembly into amyloid and other aggregates (5, 11).

Hybrid tetramers were isolated to better understand the mechanism of trans-suppression (Fig. 1A) (9). Increasing T119M subunit stoichiometry relative to V30M [or L55P (10)] shifted the maximum for acid-mediated fibril formation to a lower pH (Fig. 2A), decreased the overall yield of amyloid at physiologically accessible pH's (>4.0), and slowed the rate of acid-induced (pH 4.4)

(Fig. 2B) and methanol-mediated (10) amyloidogenesis. Several small-molecule TTR amyloid fibril inhibitors have been discovered, a subset of which were studied herein (Fig. 1B), including two drugs approved by the U.S. Food and Drug Administration (FDA) (inhibitors 8 and 10) (14). The influence of small-molecule inhibitor binding on the yield and rate of wild-type (WT) TTR fibril formation was similar to that of T119M subunit incorporation; however, the shift to a lower pH optimum for fibril formation was not observed with all the inhibitors (Fig. 2, C through E). These inhibitors function by binding to the two equivalent thyroxine (T4) sites within the TTR tetramer, not the monomer (Fig. 2F) (14–17).

Tetramer dissociation rates were measured by linking slow quaternary structural changes to the unfolding transition, with a rate of  $5 \times 10^5$  times that of dissociation (11). Denaturation-detected dissociation is irreversible because the concentration of urea used (>6.0 M) cannot support refolding. Increasing T119M subunit stoichiometry relative to the V30M [or L55P (10)] subunits revealed a dramatic TTR (1.8 μM) tetramer dissociation rate decrease (rate limiting for amyloidogenesis) in three different denaturing environments [acidic pH, aqueous methanol, or urea (Fig. 3, A and B)], explaining the origin of disease prevention.

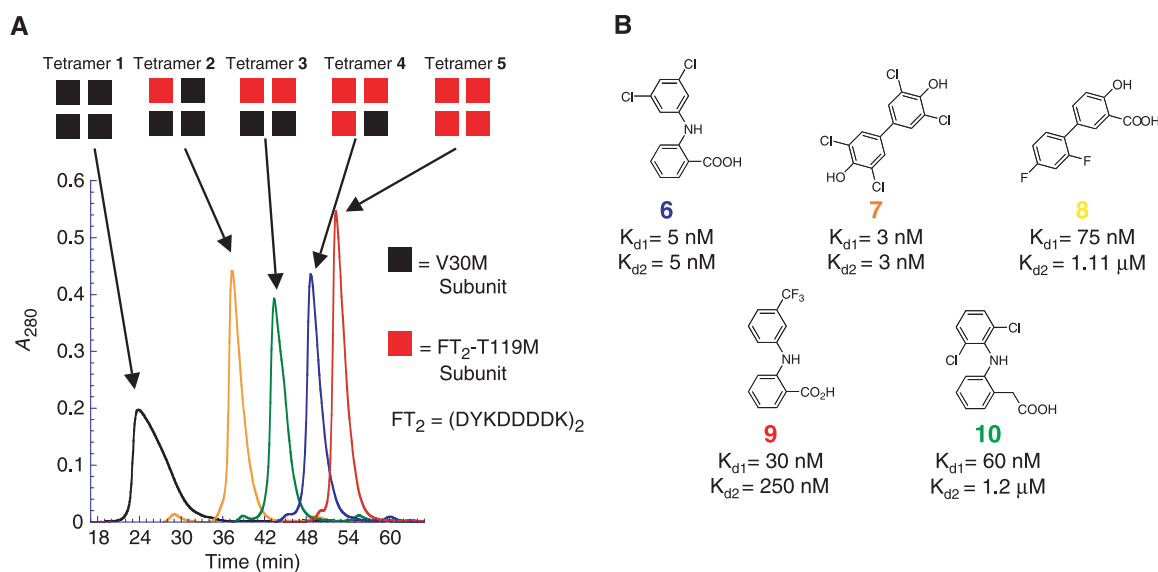
Measurements of the WT TTR tetramer (1.8 μM) dissociation rate in the presence of inhibitors 6 through 10 (1.8 and 3.6 μM) showed dose-dependent slowing for all TTR-inhibitor complexes (Fig. 3, C and D). The initial rate of tetramer dissociation was roughly inversely proportional to the mole fraction of the tetramer bound to two inhibitors ( $T \cdot I_2$ ). In the case of inhibitors 6, 7, and

Department of Chemistry and The Skaggs Institute of Chemical Biology, The Scripps Research Institute, 10550 North Torrey Pines Road, La Jolla, CA 92037, USA.

\*These authors contributed equally to this work.

†To whom correspondence should be addressed. E-mail: jkelly@scripps.edu

**Fig. 1. (A)** Anion exchange chromatogram of tetramers 1 through 5 composed of V30M (black subunits) and FT<sub>2</sub>-T119M (red subunits) (D, Asp; Y, Tyr; K, Lys). Hybrid tetramers were produced by coexpression in *Escherichia coli* (9). A<sub>280</sub>, absorbance at 280 nm. **(B)** Structure and dissociation constants (K<sub>d1</sub> and K<sub>d2</sub>) for the small-molecule inhibitors (6 through 10). The structure number colors correlate with the data presented in Fig. 2, C through F, and Fig. 3, C through E. The dissociation constants of 6 and 8 were determined by isothermal titration calorimetry at pH 7.0 (25°C), analogous to 7, 9, and 10 (30–32).



## REPORTS

**Fig. 2.** Time- and pH-dependent TTR (3.6  $\mu\text{M}$ ) amyloid fibril formation as a function of trans-suppressor subunit stoichiometry or small-molecule inhibitor binding. **(A)** Amyloid formation from tetramers 1 through 5 as a function of pH (72 hours, 37°C). Bar colors for tetramers are as follows: 1, black; 2, orange; 3, green; 4, blue; and 5, red. **(B)** Time course of amyloid fibril formation (pH 4.4, 37°C) from tetramers 1 through 5; the color scheme is as in (A). **(C and D)** WT TTR fibril formation as a function of pH (72 hours, 37°C) and inhibitor concentration [3.6  $\mu\text{M}$  (C) or 7.2  $\mu\text{M}$  (D)] versus control in the absence of inhibitor (black bars); the inhibitor color scheme is as in Fig. 1B. **(E)** Time courses of acid-mediated WT TTR fibril formation in the presence of inhibitors (3.6  $\mu\text{M}$ , pH 4.4); color scheme is as in Fig. 1B. **(F)** Time courses of acid-mediated M-TTR (pH 4.4) fibril formation in the presence of inhibitors 6 through 10 (7.2  $\mu\text{M}$ ); color scheme is as in Fig. 1B (24).

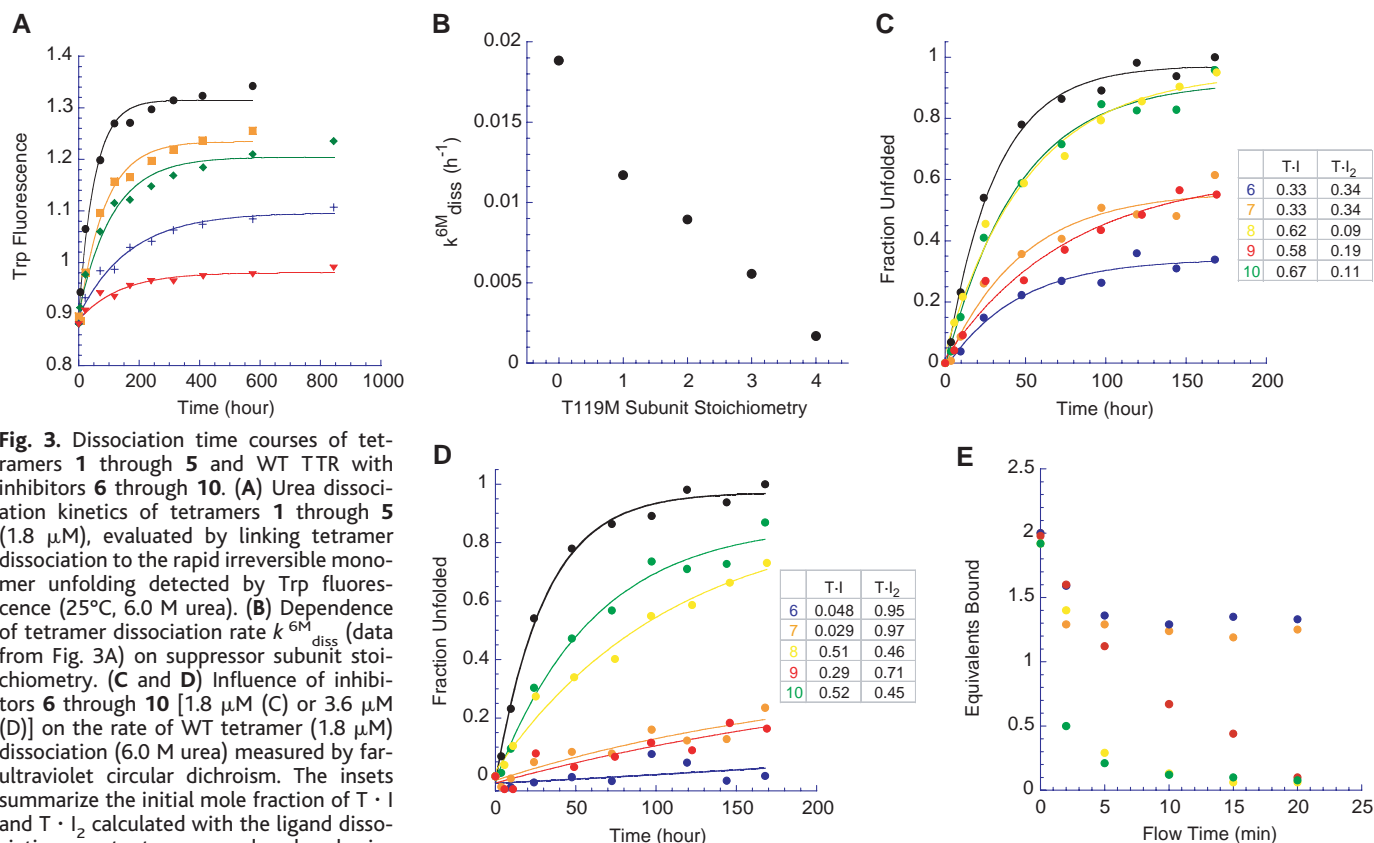
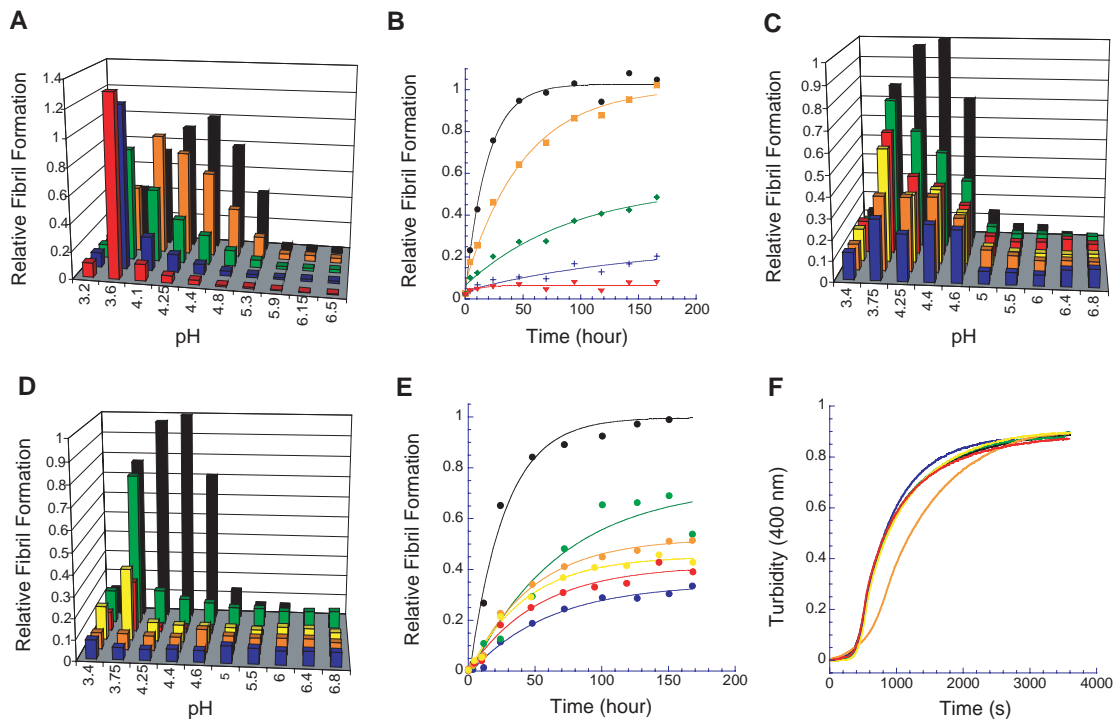


**Fig. 3.** Dissociation time courses of tetramers 1 through 5 and WT TTR with inhibitors 6 through 10. **(A)** Urea dissociation kinetics of tetramers 1 through 5 (1.8  $\mu\text{M}$ ), evaluated by linking tetramer dissociation to the rapid irreversible monomer unfolding detected by Trp fluorescence (25°C, 6.0 M urea). **(B)** Dependence of tetramer dissociation rate  $k^{\text{diss}}_{6\text{M}}$  (data from Fig. 3A) on suppressor subunit stoichiometry. **(C and D)** Influence of inhibitors 6 through 10 [1.8  $\mu\text{M}$  (C) or 3.6  $\mu\text{M}$  (D)] on the rate of WT tetramer (1.8  $\mu\text{M}$ ) dissociation (6.0 M urea) measured by far-ultraviolet circular dichroism. The insets summarize the initial mole fraction of T · I and T · I<sub>2</sub> calculated with the ligand dissociation constants measured under physiological conditions (Fig. 1B). The color scheme is as in Fig. 1B. **(E)** Relative inhibitor dissociation rates were evaluated by flowing aqueous solution over T · I<sub>2</sub> immobilized with a TTR polyclonal antibody linked to a resin (33). Binding stoichiometry was ascertained by a high-performance liquid chromatography assay, described previously (33).

**9** (1.8  $\mu\text{M}$ ) (Fig. 3C), the amplitude of the single exponential correlated primarily with dissociation of the unliganded tetramer (and, to a lesser extent,  $\text{T} \cdot \text{I}$ ), implying that  $\text{T} \cdot \text{I}_2$  prevented tetramer dissociation in 6 M urea (18). In contrast, formation of  $\text{T} \cdot \text{I}$  and  $\text{T} \cdot \text{I}_2$  for inhibitors **8** and **10** did not protect the tetramer substantially from dissociation in urea, revealing that binding alone was insufficient. The efficient inhibition observed in the case of **6**, **7**, and **9** (3.6  $\mu\text{M}$ ) resulted from the binding energy stabilizing the  $\text{T} \cdot \text{I}_2$  complex by free energies exceeding 2.3 kcal/mol (Fig. 4A) (19). Stabilizing  $\text{T} \cdot \text{I}_2$  relative to  $\text{T}$  by 2.7 kcal/mol would translate to a two-order-of-magnitude decrease in the rate of TTR tetramer dissociation (Fig. 4A). The strong negatively cooperative binding (Fig. 1B) of inhibitors **8** and **10** (3.6  $\mu\text{M}$ ) dictates that binding to the second site ( $\text{T} \cdot \text{I}_2$ ,  $\mu\text{M}$  dissociation constants) would not further stabilize TTR relative to binding to the first site ( $\text{T} \cdot \text{I}$ ) (Fig. 4A). The nM dissociation constants ( $K_{d1}$  and  $K_{d2}$ ) of inhibitors **6**, **7**, and **9** would ensure that ground-state stabilization ( $>2.3$  kcal/mol) would be sufficient to substantially increase the activation barrier for TTR tetramer dissociation, provided that the inhibitors did not bind to and similarly stabi-

lize the dissociative transition state. The inhibitor dissociation rates from the  $\text{T} \cdot \text{I}_2$  and  $\text{T} \cdot \text{I}$  complex could also play a role in the efficacy of inhibitors **6**, **7**, and **9** (20). TTR saturated with inhibitor was immobilized by an antibody resin, over which aqueous buffer was passed at 5.0 ml/min to evaluate effective dissociation rates of **6** through **10**. The best inhibitors were those with the lowest apparent dissociation rates (Fig. 3E).

Although there is generally a very good correlation between the amyloidogenesis rates (acidic conditions) and tetramer dissociation rates (in urea) in the presence of inhibitors, this need not be the case. Amyloidogenesis requires concentration-dependent misassembly after dissociation. Thus, small molecules will generally be more effective at preventing fibril formation than tetramer dissociation, especially when the inhibitor can keep the concentration of the monomeric amyloidogenic intermediate low ( $<3.6$   $\mu\text{M}$ ), where fibril formation is very inefficient (compare Figs. 2E and 3C). Occasionally, tetramer dissociation rates measured in urea will not accurately predict the rank ordering of inhibitor efficacy under acidic conditions. For example, the FDA-approved drug diflunisal (**8**) was a much better amyloid inhib-

itor than a tetramer dissociation inhibitor (compare Figs. 2E and 3C). A likely explanation for this observation is that  $K_{d1}$  and/or  $K_{d2}$  are lower in acid than in urea (18). In addition, some inhibitors perform much better under denaturing conditions than their binding constants determined under physiological conditions would suggest. For example, compound **9** was more or equally efficient at preventing tetramer dissociation (urea) and fibril formation (acid) than was inhibitor **7**, despite inhibitor **9** having  $K_{d1}$  and  $K_{d2}$  values that were 10 and 83 times that of **7**, respectively (measured under physiological conditions). Thus, it is important to judge the efficacy of misfolding inhibitors under a variety of denaturing conditions and not just under physiological conditions.

Inclusion of T119M trans-suppressor subunits into tetramers otherwise composed of disease-associated subunits could decrease the rate of tetramer dissociation by stabilizing the tetrameric ground state to a greater extent than the transition state (as is the case with the small-molecule inhibitors) and/or by destabilizing the transition state of dissociation. To distinguish between these possibilities, we compared the reconstitution kinetics of WT and T119M homotetramers. Refolding of T119M monomers was rapid and within error of the folding rate of WT TTR monomers (10); however, reassembly of T119M folded monomers was two orders of magnitude slower than the tetramerization of WT TTR monomers initiated by urea dilution (11). The reassembly process is biphasic, which can be explained by the presence of an observable intermediate in the assembly pathway (probably a dimer). In the opposite direction, the T119M tetramer dissociates at 1/37 the rate exhibited by the WT TTR tetramer (11). These kinetic effects cannot be attributed to differences in tertiary structural stability and/or tetramer stability. A direct comparison of the thermodynamic stability of WT and T119M monomers [employing an engineered monomeric TTR construct (M-TTR) (10)] revealed a difference in the free energy  $\Delta\Delta G$  for unfolding of only 0.4 kcal/mol, much less than the 2.1 and 2.7 kcal/mol required to explain the dissociation and assembly rate differences, respectively. A thermodynamic cycle analysis of T119M and WT TTR revealed that T119M prevents dissociation of the tetramer by destabilizing the dissociation transition state by  $\approx 3.1$  kcal/mol (Fig. 4, B and C), not by tetramer stabilization. According to this analysis, the T119M tetramer is actually destabilized by 0.9 kcal/mol relative to WT, further supporting a kinetic stabilization mechanism (21). The free-energy difference between WT and T119M tetramer dissociation cannot be measured through urea-mediated unfolding because T119M denaturation in urea requires exceedingly long incubation

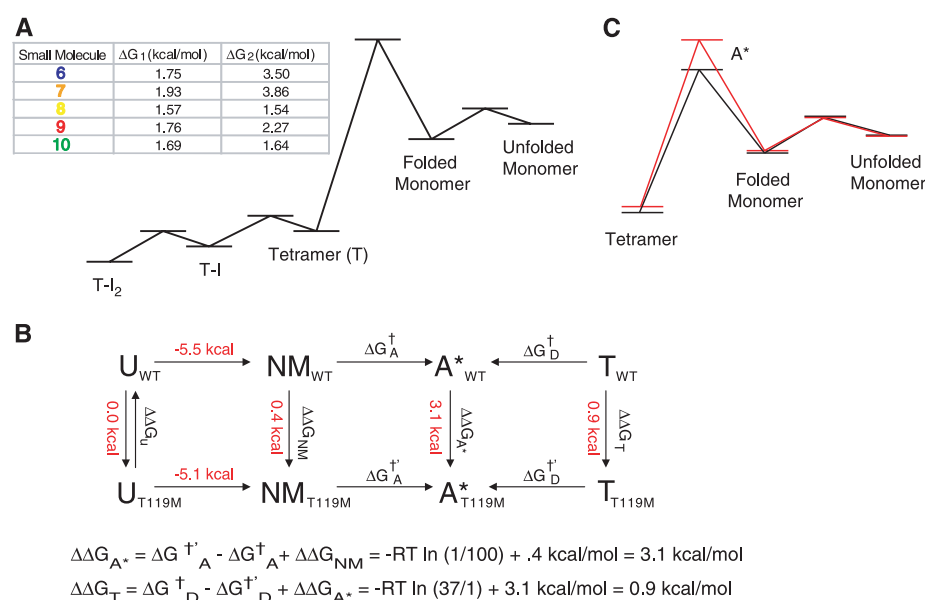


**Fig. 4.** Energy landscape depictions of the mechanism by which T119M trans-suppression and the small-molecule inhibitors function to prevent TTR amyloid fibril formation. (A) Inhibitor binding to TTR increases the activation barrier associated with tetramer dissociation through tetramer stabilization. The table summarizes the extent of TTR stabilization imparted by binding inhibitors **6** through **10**.  $\Delta G_1$  and  $\Delta G_2$  refer to the free energy of stabilization resulting from the binding of one and two equivalents, respectively, of inhibitor (3.6  $\mu\text{M}$ ) to TTR (1.8  $\mu\text{M}$ , 25°C) (19). (B) Thermodynamic cycle analysis of T119M and WT TTR displaying the energetic differences. U refers to the unfolded state, NM is the native monomer,  $A^*$  refers to the activated state or transition state associated with tetramer dissociation, T represents the tetramer, and subscripts distinguish WT from T119M. The  $\dagger$  refers to activation parameters for WT TTR, and the  $\dagger'$  refers to the same for T119M. Subscripts D and A refer to dissociation and association, respectively. The equations presented are those that were used to calculate the values in the thermodynamic cycle analysis. (C) T119M (red) tetramers have an  $A^*$  energy that is higher than that of WT (black), demonstrating that the T119M subunits increase the kinetic barrier of tetramer dissociation largely through transition-state destabilization.

## REPORTS

periods [several weeks (11)], during which TTR becomes modified. Comparisons of guanidinium chloride (GdmCl) and guanidinium thiocyanate (GdmSCN) denaturation curves revealed that WT TTR was more resistant to GdmCl denaturation than was T119M, whereas the opposite was true in GdmSCN, as shown previously (9). These differences in midpoints of denaturation can be attributed to differential anion stabilization, suggesting that the true thermodynamic stabilities of these proteins are very similar, although a quantitative analysis is not possible in these chaotropes (22).

A free-energy landscape diagram consistent with all of the experimental data relevant to T119M trans-suppression is shown in Fig. 4C. T119M trans-suppression is principally mediated by destabilization of the dissociative transition state, consistent with positioning of T119M at the dimer-dimer interface. Increasing the dissociative transition-state energy by 3.1 kcal/mol effectively prevents tetramer dissociation because the activation barrier becomes insurmountable (dissociation half-life  $t_{1/2}$  increases from  $\approx 42$  hours to  $>1500$  hours). Small-molecule binding similarly increases the activation barrier associated with tetramer dissociation in a dose-dependent fashion, although this is mediated through tetramer stabilization (Fig. 4A). The extent of stabilization is maximal when the small-molecule dissociation constants  $K_{d1}$  and  $K_{d2}$  are as low as possible and the concentration of inhibitor is as high as possible. The concentrations used in our experiments for ground-state stabilization are comparable to those observed in plasma for numerous orally available drugs.

Small-molecule binding and trans-suppression increase the activation energy associated with tetramer dissociation, the rate-limiting step of TTR fibril formation. Establishing this analogy is important because it is known that trans-suppression prevents disease in V30M compound heterozygotes (7, 8). Kinetic stabilization of the native state is a particularly attractive strategy, considering the emerging evidence that small misfolded oligomers are neurotoxic (23). Discovering small-molecule binders or developing a trans-suppression approach to tune the energy landscape of other pathologically relevant proteins with a predilection to misfold should now be considered.

### References and Notes

1. C. M. Dobson, *Trends Biochem. Sci.* **24**, 329 (1999).
2. A. L. Fink, *Folding Des.* **3**, R9 (1998).
3. D. J. Selkoe, *Science* **275**, 630 (1997).
4. M. S. Goldberg, P. T. Lansbury Jr., *Nature Cell Biol.* **2**, E115 (2000).
5. J. W. Kelly, *Curr. Opin. Struct. Biol.* **6**, 11 (1996).
6. D. R. Jacobson, J. N. Buxbaum, *Adv. Hum. Genet.* **20**, 69 (1991).
7. T. Coelho et al., *J. Rheumatol.* **20**, 179 (1993).
8. T. Coelho et al., *Neuromuscular Disord.* **6**, 27 (1996).

9. P. Hammarström, F. Schneider, J. W. Kelly, *Science* **293**, 2459 (2001).
10. Supporting material is available on Science Online.
11. P. Hammarström, X. Jiang, A. R. Hurshman, E. T. Powers, J. W. Kelly, *Proc. Natl. Acad. Sci. U.S.A.* **99**, 16427 (2002).
12. S. L. McCutchen, Z. Lai, G. Miroy, J. W. Kelly, W. Colon, *Biochemistry* **34**, 13527 (1995).
13. X. Jiang, J. N. Buxbaum, J. W. Kelly, *Proc. Natl. Acad. Sci. U.S.A.* **98**, 14943 (2001).
14. J. C. Sacchettini, J. W. Kelly, *Nature Rev. Drug Discovery* **1**, 267 (2002).
15. G. J. Miroy et al., *Proc. Natl. Acad. Sci. U.S.A.* **93**, 15051 (1996).
16. Small-molecule inhibitors **6** and **8** through **10** do not inhibit TTR amyloidosis when a monomeric variant of TTR (M-TTR) (24) is employed for acid-mediated amyloid fibril formation studies (Fig. 2F), demonstrating that the inhibitors mediate amyloid inhibition through tetramer binding (Fig. 2, E and F). Inhibitor **7** slightly inhibits fibril formation from M-TTR because it drives a small fraction of M-TTR into a tetrameric quaternary structure (Fig. 2F).
17. T. Klabunde et al., *Nature Struct. Biol.* **7**, 312 (2000).
18. The calculated and observed amplitude changes do not match the populations of  $T \cdot I_1$  and  $T \cdot I_2$  displayed in Fig. 3, C and D, exactly in all cases owing to the fact that  $K_{d1}$ ,  $K_{d2}$ , and the free energy of stabilization resulting from the binding of one ( $AG_1$ ) and two ( $\Delta G_2$ ) ligands were all evaluated under physiological conditions (Fig. 1B), and the experiments described here were carried out in 6 M urea.
19.  $\Delta G_1 = RT \ln\left(\frac{[T \cdot I]/[T]}{[I]/K_{d1}}\right) = RT \ln\left(\frac{[I]}{K_{d1}}\right)$  and  $\Delta G_2 = RT \ln\left(\frac{[T \cdot I_2]/[T]}{[I]^2/(K_{d1} \cdot K_{d2})}\right)$ .
20. J. V. Schloss, *Acc. Chem. Res.* **21**, 348 (1988).
21. D. Baker, J. L. Sohl, D. A. Agard, *Nature* **356**, 263 (1992).
22. P. Hammarström, X. Jiang, S. Deechongkit, J. W. Kelly, *Biochemistry* **40**, 11453 (2001).
23. Emerging data from the laboratories of S. Lindquist (25), D. Selkoe (26), C. Dobson (27), P. Lansbury (28), G. Krafft (29), and others reveal that oligomeric aggregates of proteins with a tendency to misfold and misassemble are more toxic to cells than are the insoluble aggregates with high molecular weight (e.g., amyloid fibrils and the scrapie form of the prion protein, PrP<sup>Sc</sup>).
24. X. Jiang et al., *Biochemistry* **40**, 11442 (2001).
25. J. Ma, S. Lindquist, *Science* **298**, 1785 (2002); published online 17 October 2002 (10.1126/science.1073619).
26. D. M. Walsh et al., *Nature* **416**, 535 (2002).
27. M. Bucciantini et al., *Nature* **416**, 507 (2002).
28. H. A. Lashuel et al., *Nature* **418**, 291 (2002).
29. W. L. Klein et al., *Trends Neurosci.* **24**, 219 (2001).
30. V. B. Oza et al., *J. Med. Chem.* **45**, 321 (2002).
31. S. A. Peterson et al., *Proc. Natl. Acad. Sci. U.S.A.* **95**, 12956 (1998).
32. H. E. Purkey, J. W. Kelly, unpublished results.
33. H. E. Purkey, M. I. Dorrell, J. W. Kelly, *Proc. Natl. Acad. Sci. U.S.A.* **98**, 5566 (2001).
34. We thank NIH (grant DK 46335), The Skaggs Institute of Chemical Biology, and the Lita Annenberg Hazen Foundation for financial support; R. A. Lerner and I. Wilson for useful suggestions; and the Wenner-Gren Foundation for a postdoctoral fellowship (P.H.).

### Supporting Online Material

www.sciencemag.org/cgi/content/full/299/5607/713/DC1

SOM Text

Figs. S1 and S2

References and Notes

21 October 2002; accepted 13 December 2002

# ARGONAUTE4 Control of Locus-Specific siRNA Accumulation and DNA and Histone Methylation

Daniel Zilberman,<sup>1</sup> Xiaofeng Cao,<sup>1</sup> Steven E. Jacobsen,<sup>1,2\*</sup>

Proteins of the ARGONAUTE family are important in diverse posttranscriptional RNA-mediated gene-silencing systems as well as in transcriptional gene silencing in *Drosophila* and fission yeast and in programmed DNA elimination in *Tetrahymena*. We cloned ARGONAUTE4 (AGO4) from a screen for mutants that suppress silencing of the *Arabidopsis SUPERMAN (SUP)* gene. The *ago4-1* mutant reactivated silent *SUP* alleles and decreased CpNpG and asymmetric DNA methylation as well as histone H3 lysine-9 methylation. In addition, *ago4-1* blocked histone and DNA methylation and the accumulation of 25-nucleotide small interfering RNAs (siRNAs) that correspond to the retroelement *AtSN1*. These results suggest that AGO4 and long siRNAs direct chromatin modifications, including histone methylation and non-CpG DNA methylation.

Members of the ARGONAUTE (AGO) protein family are important in RNA-mediated silencing systems such as posttranscriptional gene silencing (PTGS) in plants, RNA interference in animals, and quelling in fungi (1, 2). These systems use a ribonuclease III enzyme, DICER, to generate 21- to 22-nucleo-

otide (nt) small interfering RNAs (siRNAs), which target the destruction of homologous RNA. In plants, PTGS is often associated with RNA-directed methylation of the corresponding DNA (3) and, conversely, plant chromatin mutants such as *ddm1* and *met1* can affect PTGS (4). In addition, AGO family members have recently been implicated in histone modifications and transcriptional gene silencing. In fission yeast, deletion of *argonaute*, *dicer*, and RNA-dependent RNA polymerase homologs causes transcriptional derepression and loss of histone H3 lysine-9

<sup>1</sup>Department of Molecular, Cell, and Developmental Biology, <sup>2</sup>Molecular Biology Institute, University of California, Los Angeles, CA 90095-1606.

\*To whom correspondence should be addressed. E-mail: jacobsen@ucla.edu.